Am J Transl Res 2017;9(12):5375-5387
www.ajtr.org /ISSN:1943-8141/AJTR0067290

Original Article

Exosomes derived from cardiac telocytes exert positive effects on endothelial cells

Jie Yang, Yanyan Li, Fengtai Xue, Wei Liu, Song Zhang

Department of Cardiovascular Diseases, Xinhua Hospital, School of Medicine, Shanghai Jiaotong University, 1665 Kongjiang Street, Shanghai 200092, P. R. China

Received July 26, 2017; Accepted November 24, 2017; Epub December 15, 2017; Published December 30, 2017

Abstract: Telocytes are novel cells that have been documented in the interstitium of multiple organs; however, their role in the heart remains unclear. This study aimed to identify cardiac telocytes by their morphological and molecular features and investigate whether their exosomes affect cardiac endothelial cells. To this end, rat cardiac telocytes were cultured and stained with methylene blue, Janus Green B, and MitoTracker green, or with antibodies for established cell surface markers, and examined by microscopy. In addition, telocyte organelles and exosome release were examined by transmission electron microscopy. To investigate exosome functions, we isolated exosomes from telocytes and co-cultured them with endothelial cells *in vitro,* as well as transfusing them into a rat model of myocardial infarction. We confirmed that cultured telocytes exhibit normal characteristics, including long, thin prolongations with a moniliform appearance, as well as positive expression of c-Kit, CD34, and vimentin. Furthermore, we observed mitochondria throughout the cell body and telopodes, and found that telocytes actively secrete exosomes. Interestingly, endothelial cells cultured with telocyte supernatants or exosomes exhibited increased proliferation, migration, and formation of capillary-like structures, and these effects were attenuated when exosomes were depleted from telocyte supernatants. Finally, treating myocardial infarction-induced rats with telocyte exosomes resulted in decreased cardiac fibrosis, improved cardiac function, and increased angiogenesis. Taken together, our results provide novel insight into cardiac telocytes, suggesting that they communicate with neighboring endothelial cells via exosome secretion and that these exosomes exert potentially beneficially effects.

Keywords: Telocytes, transmission electron microscopy, exosomes, endothelial cells, myocardial infarction

Introduction

Within the last decade, numerous research groups have investigated whether interstitial Cajal-like cells (ICLCs) are present outside the gastrointestinal tract, and their findings show unique interstitial cell populations throughout the body, including in the uterus and fallopian tube [1], trachea and lung [2, 3], skeletal muscle [4], mammary gland [5], placenta [6], brain [7], the heart [8-14], and gut. While each of these ICLC populations has been given a different name, resulting in some confusion, transmission electron microscopy (TEM) and cell culture work have revealed distinct features of these ICLCs that unequivocally distinguish them from interstitial Cajal cells, and all other interstitial cells. These features include the presence of 2-5 cell body prolongations that are very thin (less than 0.2 μm and not detectable with standard light microscopy) and extremely long (tens to hundreds of micrometers), a moniliform aspect (consisting of many dilated segments), and the presence of caveolae. Therefore, scientists have proposed the term telocytes (TCs) for this category of cells, and telopodes (Tps) for their prolongations [8].

This newly-identified cell type has been documented in the interstitium of several cavitary and non-cavitary organs [6, 8], both in humans and other vertebrates [11, 15], where they are thought to have important functions. For example, cardiac TCs differ from fibroblasts or fibrocytes, and their unique features (long, thin Tps) enable them to play nursing and guiding roles during myocardial development. Within the cardiac stem cell niche, cardiac TCs also play an essential role as niche-supporting cells that assist the cardiac stem cells and angiogenic

cells in the myocardium [16]. Furthermore, they may have important functions in regeneration following myocardial infarction (MI) [17]. However, the exact role of TCs and their mechanism of action remain unknown.

Although some studies investigating TCs have been reported in the literature, most have focused on only their histological or morphological characteristics. Therefore, the aim of this study was to perform a more in-depth investigation of TCs, including their functions, morphological characteristics, and cell surface expression. To this end, we utilized staining agents such as methylene blue, Janus Green B, and MitoTracker green to demonstrate the typical moniliform appearance of TCs. We also examined TC surface markers and compared the expression of multiple surface targets, including c-Kit, CD34, and vimentin. Using TEM, we observed that TCs actively secrete exosomes and that, when endothelial cells (ECs) were cultured in the presence of TC supernatants or exosomes isolated from TCs, ECs had increased proliferation, migration, and formation of capillary-like structures. Moreover, we found that these effects were attenuated when exosomes were first depleted from TC supernatant. After isolating exosomes from TCs, we transferred them into MI-induced rats and found decreased cardiac fibrosis, improved cardiac function, and increased angiogenesis.

Materials and methods

Animals

Six-week-old, female Sprague Dawley (150-200 g) rats (Shanghai Songlian Laboratory Animal Farms, production license SCXK2007-0011) were utilized in the present study. The rats were maintained in a qualified animal center for approximately two weeks to adapt to the new environment before being used for experiments. All the procedures for animal care, surgery and handling were performed according to the guidelines of The Ministry of Science and Technology of the People's Republic of China [(2006)398] and approved by the Shanghai Jiao Tong University Animal Care Committee.

Rats were assigned to treatment groups in a randomized manner, and experiments were double-blinded. Briefly, to induce MI, the rats were anaesthetized with sodium pentobarbital by intraperitoneal injection (50 mg/kg), intubated, and the heart exposed by separation of the ribs. Before ligation of the left anterior descending coronary artery, exosomes (200 μg) or phosphate buffered saline (PBS) was injected into the myocardium at three border zones. Exosomes were first injected 30 min before the operation, and then three additional injections were given on days 2, 4, and 6 after MI. Subsequently, the effect of exosome injections on the progression of MI was examined. Cardiac function was evaluated 28 days after treatment using a Vivid 7 dimension echocardiograph (GE, USA) with a 10 MHz central frequency scan head. All functional evaluations were conducted and analyzed by investigators blinded to the animal's treatment group. The rats were euthanized and the hearts were excised for histological analysis. Hearts were fixed in 4% paraformaldehyde, dehydrated in ethanol, embedded in paraffin, and sectioned at a thickness of 7 μm.

Preparation of cardiac TCs and ECs

Six-week-old, female Sprague Dawley (150-200 g) rats were treated with 3% pentobarbital sodium. Hearts were removed under sterile conditions and placed in 50 mL centrifuge tubes with ice-cold PBS supplemented with 1% penicillin and streptomycin (PS). The hearts were transported to the cell culture room as soon as possible. After rinsing again with fresh PBS to remove blood, the hearts were minced into millimeter-sized pieces in a sterile culture dish containing DMEM/F12 (12400-024, Gibco, Grand Island, NY, USA) supplemented with 1% PS. The pieces were washed twice and resuspended in PBS to remove the blood. Then, an enzymatic digestion medium was added and the mixture was incubated at 37°C on a shaker at 180 rpm for 40 min. The enzymatic digestion medium was a mixture of 1.5 mg/mL collagenase type 2 (V900892, Sigma, St. Louis, MO, USA), DMEM/F12, and 1% PS. The solution was filtered through a 41 μm nylon mesh (Millipore, Billerica, MA, USA) and the collected cell suspension was centrifuged at 300 *g* for 10 min. The cells were then seeded into sterile culture dishes containing 10 mL DMEM/F12, 10% exosome-depleted fetal bovine serum (FBS, SBI, USA) and 1% PS, then cultured in a humidified atmosphere at 37°C for 1 h to allow fibroblasts to attach.

The unattached cells (containing TCs) were replanted into a new dish containing the above medium, and the medium was replaced every two days thereafter. ECs were purchased from Lonza (Atlanta, GA, USA) and cultured according to the supplier's instructions. Cell cultures were examined using an inverted microscope and photographed at 72 h after seeding. The cells were detached by digestion in 0.25% trypsin/EDTA (Invitrogen, Carlsbad, CA, USA) for 1-2 min after they had grown to 70% confluence, and then reseeded at a split ratio of 1:3 under the same conditions.

Staining of TCs

The primary isolated cells were cultured in a six-well, cell culture cluster until they had grown to 70% confluence, then washed twice with PBS and incubated with 0.02% methylene blue (Sigma-Aldrich Corp., St. Louis, MO, USA), 0.02% Janus Green B (Sigma-Aldrich), and 100 nM MitoTracker green probe (Beyotime, China) in a 37°C, 5% CO_2 cell incubator for 30 min. Next, the stains were discarded and the cells were washed three times with PBS and observed microscopically.

Immunofluorescent staining

To visualize and independently confirm the appearance of isolated TCs, immunofluorescence staining was carried out on coverslips. Samples were fixed in 4% paraformaldehyde for 15 min, washed three times in PBS, and then incubated in PBS containing 5% bovine serum albumin for another 15 min. The cells or tissue were washed and permeabilized with 0.075% saponin in PBS for 10 min (all reagents from Sigma-Aldrich). Then, cells were incubated with primary antibodies: anti-vimentin (Abcam, USA), anti-C-Kit (Abcam, USA), anti-CD34 (Santa Cruz Biotechnology, USA) or anti-CD31 (Abcam, USA) at 4°C overnight in the dark. Primary antibodies were then detected with corresponding secondary antibodies conjugated to Alexa Fluor 594 (Cell Signaling Technology, USA) at 37°C for 1 h, and nuclei were counterstained with 1 μg/mL 4',6-diamidino-2-phenylindole (DAPI) to detect cell nuclei (Life Technologies, USA). Finally, the immunolabeled samples were observed and photographed under an Olympus IX83 inverted fluorescence microscope (Olympus Corp., Japan). The percentage of positively-stained cells was quantified and the average was obtained from five randomly-selected 200× fields.

TEM observation

Cell samples were processed for TEM to observe the ultrastructure of TCs. In brief, samples were fixed with 2% glutaraldehyde in PBS for 2 h at 4°C. After washing twice with PBS for 10 min, the samples were fixed in 1% phosphate buffered osmium for 2 h at 4°C. Then, the samples were dehydrated in an increasing ethanol series (30%, 50%, 70%, 80%, 95%, 100%), cleared with propylene oxide and embedded in Araldite resin. Thin sections were obtained and stained with lead citrate. The sections were examined with a transmission electron microscope (FEI Company, Eindhoven, Netherlands). Digital electron micrographs were recorded with a MegaView III charge-coupled device using iTEM SIS software (Olympus Soft Imaging Systems, Munster, Germany).

Exosome preparation

Supernatants from cultured TCs were collected on ice and centrifuged at 10,000×g for 30 min to remove any cells and cellular debris. Then, supernatants were transferred to a fresh tube, filtered through a 0.22 μm membrane, and centrifuged at 120,000×g for 2 h at 4°C. The isolated exosomal pellet was washed once with sterile PBS and resuspended in 200 μL of PBS. Alternatively, in some samples the supernatants were first concentrated by decreasing the volume from 50 mL to 1 mL using an Amicon Ultra filter (Millipore, USA) with a 100,000 molecular weight cutoff. Subsequently, exosomes were isolated from the concentrated supernatants using an ExoQuick kit (SBI, USA), per the manufacturer's instructions.

The quality of exosomes was confirmed by qNano analysis (Izon instrument, UK), according to the manufacturer's instructions. Protein content of the exosome pellet fraction was quantified using the BCA Protein Assay Kit (Thermo Fisher Scientific, USA). All samples were measured in triplicate.

Electron microscopy was performed as previously described [18]. Briefly, exosomes were ultra-centrifuged to generate a pellet as part of the final step of isolation. A drop of purified exosome pellet was allowed to settle on a gold-

coated grid, blotted, fixed in 1% glutaraldehyde, washed for 2 min in double-distilled water, and incubated in uranyl oxalate for 5 min. Subsequently, it was incubated in three separate drops of methyl cellulose with uranyl acetate (5 min in the first two drops and 10 min in the last drop), and finally removed from methyl cellulose-uranyl acetate by slowly dragging it on the edge of a filter paper. Exosomes were visualized by standard TEM with a Philips CM120 microscope.

Exosome labeling

Exosomes were labeled with a phospholipid membrane dye, PKH26 (Sigma, USA) at 37°C for 5 min, per the manufacturer's instructions. Briefly, exosomes (10^{10} particles) were resuspended in 100 μL of PBS, then 0.5 mL diluent C was added, followed by a mixture of 4 μL PKH26 and 0.5 mL diluent C, and allowed to react for 5 min. Exosome-depleted FBS (1 mL) was added to stop the reaction and the solution was transferred to a fresh tube, filtered through a 0.22 μm membrane, and centrifuged at 120,000×g for 2 h at 4°C. The PKH26-labeled exosomes were resuspended in basal medium and added to cultured ECs which were transfected with a lentiviral vector designed to induce GFP overexpression. After incubation for 12 h, ECs were fixed, washed, and viewed under an Olympus microscope.

In some experiments, TCs were transfected with a lentiviral vector designed to induce cel-miR-39 overexpression. Then, exosomes from these TCs were isolated and added to ECs. After incubation for 4, 8, 12, or 24 h, the expression of cel-miR-39 in ECs was measured. To further investigate the role of exosomes, we depleted TCs of exosomes through ultracentrifugation or by using 14 μM of GW4869 (an inhibitor of exosome release) (Sigma, USA).

RNA isolation and quantitative real-time polymerase chain reaction

Total RNA was extracted using the TRIzol reagent (Invitrogen), according to the manufacturer's protocol. To quantify cel-miRNA-39, the Bulge-Loop miRNA qPCR Primer Set (RiboBio, China) was used to determine miRNA expression with Takara SYBR Premix Ex Taq (Tli RNaseH Plus) reagent. The relative expression levels among groups were calculated by the $2^{-\Delta\Delta Ct}$ method.

Western blotting

Western blotting was used to confirm the identity of exosomes, which are characterized by the absence of calnexin and the presence of the specific surface proteins CD9, CD63, and Alix [19]. Briefly, 5× protein-loading buffer was added to the exosome sample and heated at 95°C for 5 min. Next, exosome protein was resolved by electrophoresis on 12% sodium dodecyl sulfate/polyacrylamide gels. The protein sample was run at 120 V for 45 min and transferred onto polyvinylidene difluoride membranes (Millipore, USA) for 1.5 h at 100 mA. The following antibodies were used: anti-Alix, anti-CD9, anti-CD63, anti-CD81, anti-HSP90, anti-TSG101 and anti-calnexin (all from Abcam, USA). The membranes were washed three times in 1× Tris-HCl buffered saline with 0.1% Tween 20 (TBST) for 5 min, then incubated for 1 h in TBST containing horseradish peroxidase-conjugated secondary antibody (Abcam, USA). Proteins were detected using enhanced chemiluminescence (Thermo Fisher, USA) and imaged using an ImageQuant LAS 4000 mini biomolecular imager (Bio-Rad, USA). Western blot normalized to β-actin (Abcam, USA).

MTS assay

EC proliferation was assessed using an MTS assay (CellTiter 96 AQueous One Solution Cell Proliferation Assay Kit, Promega, USA), per the manufacturer's instructions. ECs were seeded into 96-well plates at an initial density of 5×10^3 cells/well. After 2 h, exosomes were added for an additional 24 h. A curve representative of cell proliferation was constructed by measuring cell growth with a microplate reader at 490 nm.

Migration analysis

A total of 10^6 ECs were seeded into a six-well plate and incubated at 37°C until 60% confluence. Then, the cells were treated with the supernatant of TCs or exosomes from TCs for another 24 h, and migration distance was observed by microscope.

Capillary-like structure formation assay

Briefly, 10^4 ECs were pretreated with the supernatant of TCs or exosomes from TCs for 24 h and seeded into Matrigel-coated 96-well plates. Following 6 h of incubation at 37°C, images

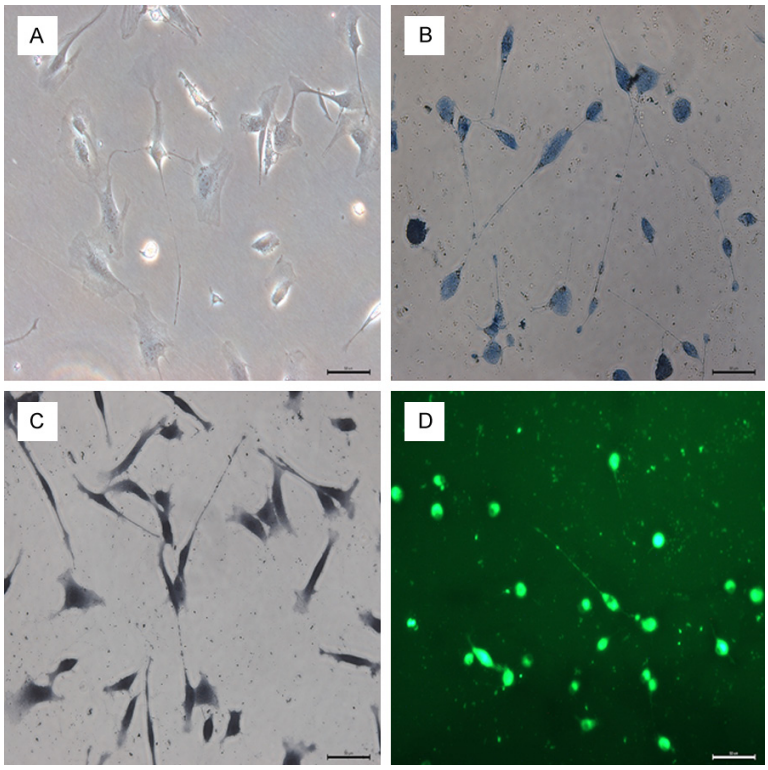

Figure 1. Representative images of live, cultured telocytes (TCs). Primary isolated cells were cultured until they reached 70% confluence, stained, and observed with light microscopy. A. TCs were very long and very thin (< 0.2 μm), with a moniliform appearance of thin segments and alternating dilations. B. Methylene blue staining of TCs reveals that they are connected through their telopodes. C, D. TCs were stained with Janus Green B and with MitoTracker green probe to label mitochondria. Mitochondria are seen throughout the cell body and telopodes with both stains. Scale bar: 50 μm.

were acquired under an Olympus microscope. Each assay was repeated five times.

Masson's trichrome staining

Tissue sections were dewaxed in Histo-Clear agent (National Diagnostics, USA) followed by a series of washes in ethanol, then stained with Masson's solution for 1 h (Sigma, USA). The sections were washed in acidified water and ethanol and mounted in Cytoseal resinous medium (Thermo Fisher, USA). Fibrosis was quantified using Image J software and expressed as the ratio of fibrotic tissue to total tissue.

Collagen content analysis

Each heart sample was weighed, homogenized with pepsin, and then collagen content was measured using the Sircol assay (Biocolor, UK), according to the manufacturer's instructions. Gen5 Software (BioTek, USA) was used to quantify collagen content.

Statistics

Statistics were calculated with GraphPad Prism software. An unpaired Student's *t*-test was used to compare two groups, where appropriate. A one-way analysis of variance was followed performed, by post-test analysis using the Tukey test, for multiple comparisons. A two-way analysis of variance was carried out, followed by Bonferroni correction, to test for significance when performing multiple comparisons between different groups. *P* values less than 0.05 were considered to indicate statistically significant differences.

Results

Staining of cultured cardiac TCs show a unique appearance

After isolation, purification, and culturing, the morphological characteristics of TCs were observable under light microscopy (**Figure 1A**). Consistent with the literature, we found them to have Tps that were very long and thin (< 0.5 μm), with a moniliform appearance: thin segments (podomeres) and alternating dilations (podoms). Interestingly, after staining with methylene blue (**Figure 1B**), we observed that the TCs were connected to one another directly through their Tps, which might be how they conduct intracellular signaling. Next, we stained the cells with Janus Green B (**Figure 1C**) or with MitoTracker green (**Figure 1D**), which stain intracellular mitochondria supravitally. As shown in **Figure 1C** and **1D**, we found that TCs contain a large number of mitochondria, which could suggest that TCs produce and consume a great deal of energy.

Cardiac TCs were c-Kit, CD34, and vimentin positive

Immunofluorescence of the isolated cells revealed positive expression of c-Kit, CD34, and vimentin, which are markers for TCs (**Figure 2**). In addition, we quantified the percentage of

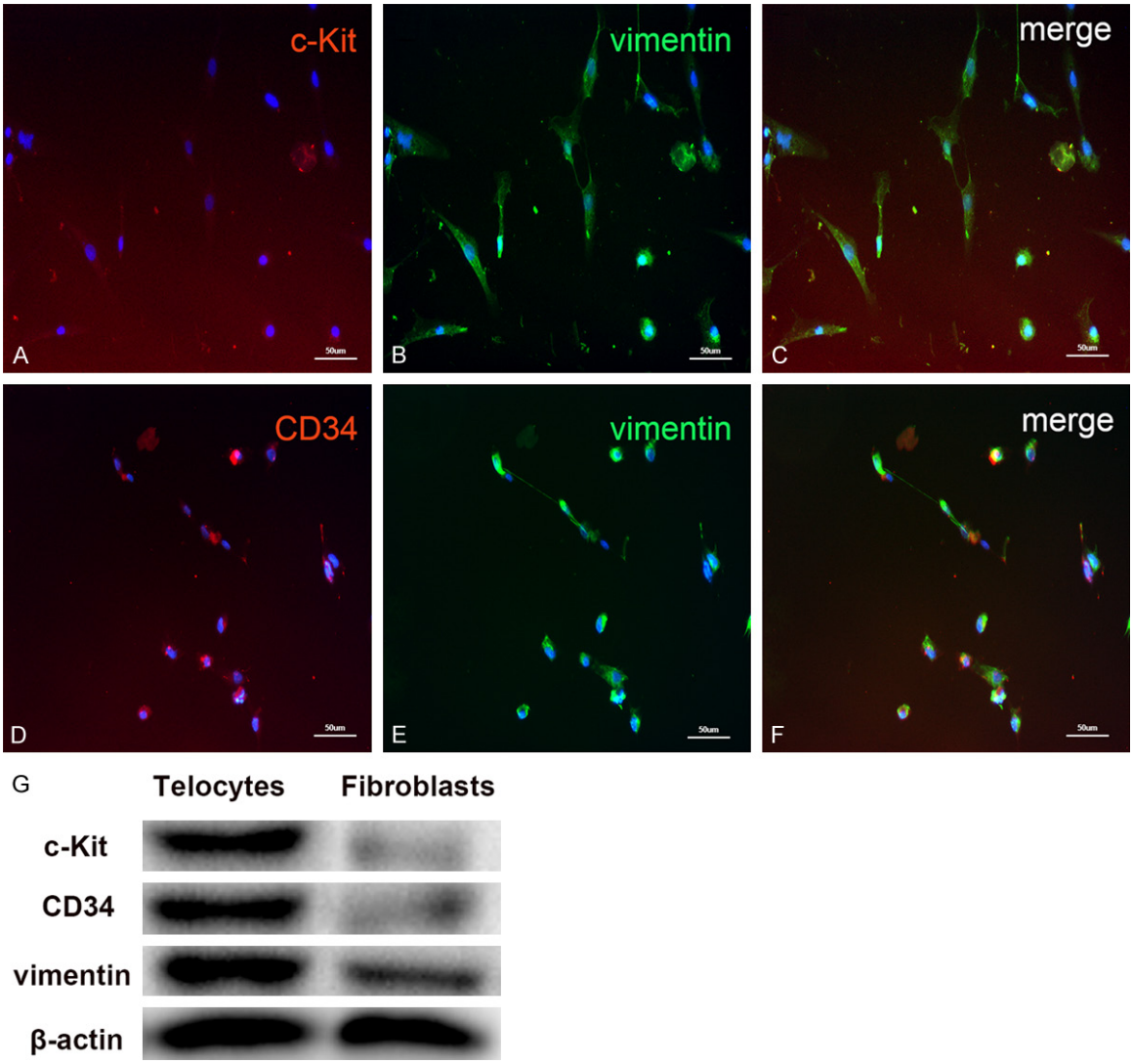

Figure 2. Representative images of rat cardiac telocytes (TCs) with fluorescence microscopy. Cells were cultured for 72 h and, after one passage, fixed in 4% paraformaldehyde and stained with known TC markers, as well as DAPI to label cell nuclei (blue). Observation with an immunofluorescent microscope revealed that the isolated cells positively expressed (A) c-Kit (red) and (B) vimentin (green). (C) Co-staining of vimentin and c-Kit is observed by merging the two images. (D) TCs positively expressed CD34 (red) and co-staining with (E) vimentin (green) showed many cells stained positive for both upon (F) merging the images. Scale bar: 50 μm. (G) Comparison of TC markers with that of fibroblasts. The proteins of cells were separated by SDS-PAGE, and electroblotted to the polyvinylidene (PVDF) membrane, and probed with relative markers. β-actin was used as a loading control.

positively-stained cells (as the average of five, randomly-selected fields) and found that more cells were positively co-stained for CD34 and vimentin than for c-Kit and vimentin (87.2% ± 12% *vs*. 70.5% ± 10%, respectively, $P < 0.05$, $n = 5$). These were also confirmed by western blot (**Figure 2G**).

TC observation by TEM

We utilized TEM to examine the characteristics of organelles within interstitial cardiac TCs in cell culture. We observed long, thin cellular processes (Tps) and a thin layer of cytoplasm surrounding the nucleus (**Figure 3A**). In addition, TCs exhibited a prominent nucleus, as well as numerous mitochondria and multivesicular bodies (enclosed by black circles, **Figure 3B**), which contain intraluminal vesicles from which exosomes are derived. When multivesicular bodies fused with the plasma membrane, exosomes were released. Notably, ectosomes were frequently observed near pits, which sug-

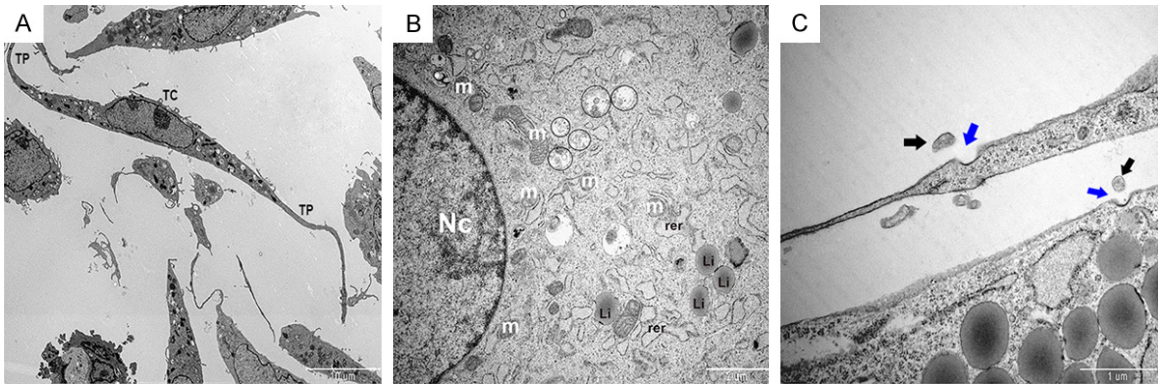

Figure 3. Observation of telocyte (TC) organelles by transmission electron microscopy. A. Representative image showing the general appearance of TCs. Scale bar: 10 μm. B. The major organelles within a TC are shown and labeled as follows: Nc, nucleus; m, mitochondria; rer, rough endoplasmic reticulum; Li, lipid particle. Scale bar: 2 μm. Multivesicular bodies are enclosed by black circles. C. Representative image of a TC actively secreting exosomes. Black arrows indicate exosomes and blue arrows indicate pits. Scale bar: 1 μm.

gest receptor-mediated endocytosis of these vesicles (**Figure 3C**).

Exosome isolation and identification

We next investigated whether exosomes play a role in crosstalk between TCs and ECs. To this end, we isolated exosomes from TCs and performed a combination of TEM, Western blotting, and a nanoparticle tracking analysis to confirm their identity. Observations using TEM revealed that isolated exosomes, which appeared as cup- or round-shaped vesicles, ranged from approximately 30 to 200 nm in diameter (**Figure 4A**). Comparison of exosomal preparations with cell lysates by immunoblotting revealed an enrichment of the exosomal markers Alix, CD9, CD63, HSP 90, CD 81 and TSG101, but the absence of calnexin (an endoplasmic reticulum protein) and β-actin (a protein encoded by host gene of cells) (**Figure 4B** and **4C**). The quality of exosomes was confirmed by qNano analysis, which showed that the diameter of most exosomes ranged from 50 to 150 nm (**Figure 4D**).

Once we had confirmed that we had successfully isolated exosomes, we investigated whether exosomes released by TCs can be transferred to recipient ECs by labeling isolated exosomes with the fluorescent dye PKH26. We then added the labeled exosomes to the culture medium of GFP-labeled ECs. After 12 h of incubation, confocal imaging showed that the ECs had taken up the fluorescently labeled exosomes (**Figure 4E**). To confirm these findings, we transfected TCs with a microRNA that is naturally present only in *Caenorhabditis elegans* (cel-miR-39). Forty-eight hours later, exosomes from cel-miR-39-transfected TCs were isolated and added to ECs. Analysis of cel-miR-39 expression demonstrated the presence of cel-miR-39 in ECs, and that the transfer from TCs to ECs occurred in a time-dependent manner (**Figure 4F**).

Exosomes from TCs exert positive effects on ECs

To determine the effects of exosomes from TCs on ECs, we co-cultured ECs with either supernatant from cultured TCs or supernatant from ECs (**Figure 5**). We observed a significant increase in proliferation, migration, and the formation of capillary-like structures by ECs when they were cultured with TC supernatant. Moreover, these effects were comparable to those observed when 20 μg/mL of TC exosomes were added to ECs. However, depletion of exosomes from TCs, through ultracentrifugation or by treatment with GW4869, considerably abrogated the effects of their supernatant on target ECs.

Effects of exosomes in vivo after MI

Finally, to assess the effects of exosomes on MI, we administered exosomes from TCs to MI rats via myocardial injection. Compared with the PBS negative control group, exosomes from TCs improved cardiac function, as shown by echocardiography (**Figure 6A**). Importantly,

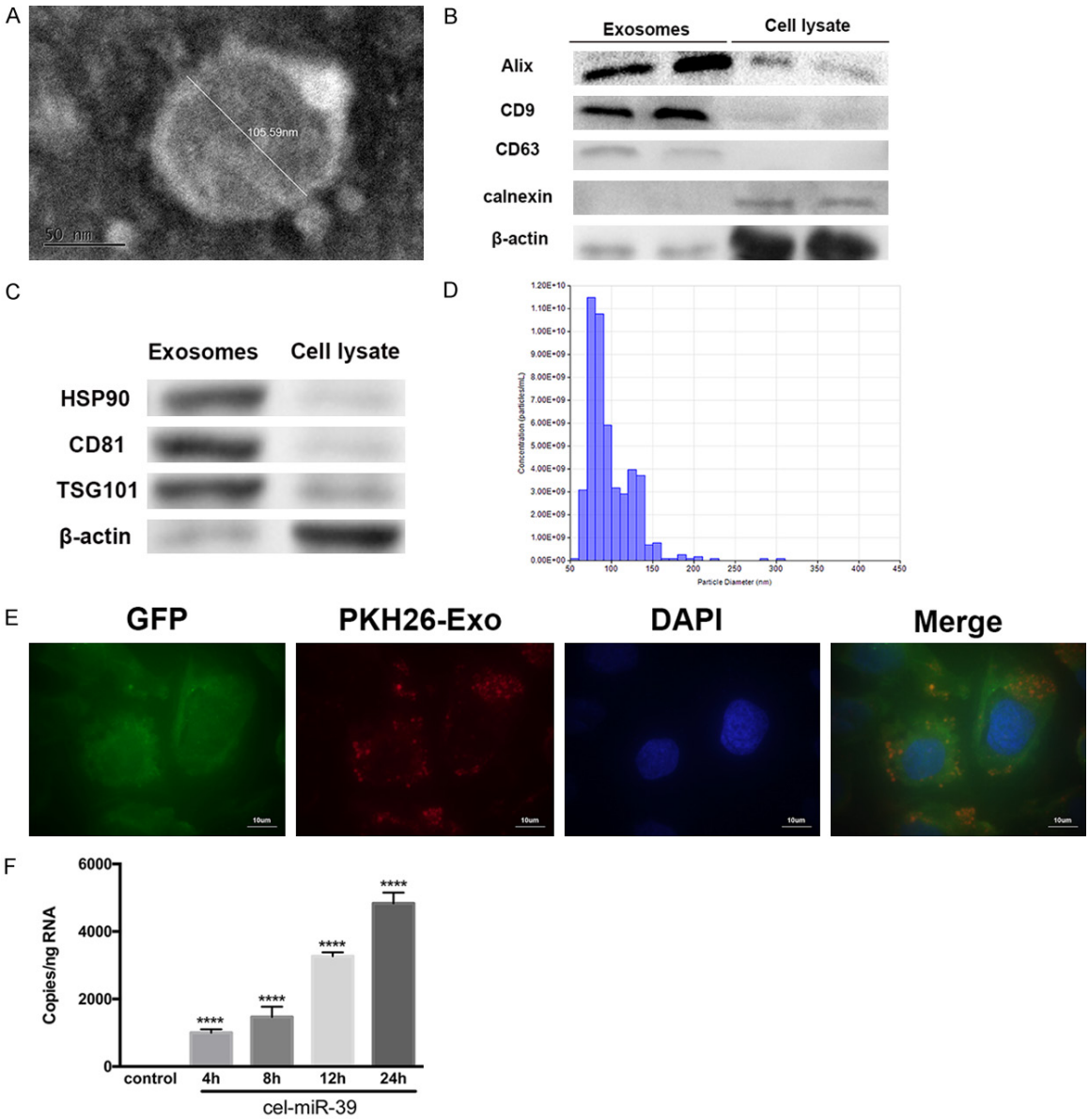

Figure 4. Isolation of exosomes from telocytes (TCs) and investigation of their uptake by endothelial cells (ECs). A. Representative electron microscopy image of TC exosomes. The diameter of this exosome was measured to be 105.59 nm. Scale bar: 50 nm. B, C. To confirm their identity, exosomal preparations were compared with cells lysates by Western blotting. The blot shown an enrichment of the exosomal markers Alix, CD9, CD63, HSP90, CD81 and TSG101 but the absence of calnexin, an endoplasmic reticulum protein. β-actin was used as a loading control. D. Exosome identity was further confirmed with a qNano analysis, which measured the diameters of the particles with respect to concentration. Most particles ranged from 50 to 150 nm in diameter. E. Isolated exosomes from TCs were labeled with PKH26 (red) and added to the culture medium of GFP-labeled ECs (green). After 12 h, cells were stained with DAPI (blue) to label cell nuclei and confocal imaging showed that the exosomes were present in the cytoplasm of ECs. Scale bar: 10 μm. F. TCs were transfected with cel-miR-39 or left un-transfected (control). Cultured ECs were then treated with exosomes isolated from control or cel-miR-39-transfected TCs for the indicated times. The RNA levels of cel-miR-39 were then measured in ECs using RT-PCR. ****, $P < 0.0001$ *versus* control; $n = 5$.

Masson's trichrome staining and collagen content analysis showed that transferring exosomes attenuated cardiac fibrosis (**Figure 6B**) and reduced collagen deposition (**Figure 6C**) in post-MI heart tissues. Lastly, transferred exosomes resulted in increased angiogenesis, as evidenced by increased staining for CD31 (**Figure 6D**).

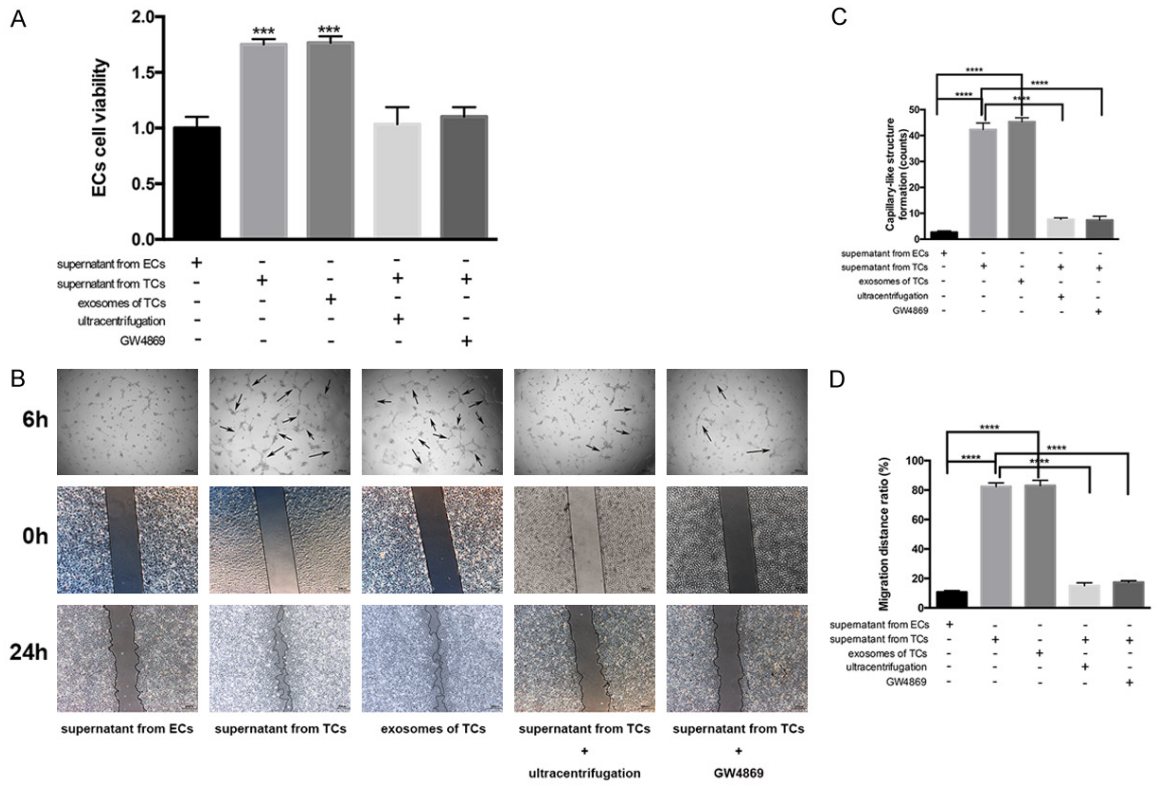

Figure 5. Culturing endothelial cells (ECs) in the presence of supernatant from telocytes (TCs) induces positive effects that are mediated by exosomes. ECs were cultured in the presence of supernatant from ECs (control), supernatant from TCs, or isolated exosomes (20 μg/mL) from TCs. In addition, some ECs were cultured with supernatant from TCs that had been depleted of exosomes by either ultracentrifugation or treatment with GW4869. A. Proliferation of ECs under each condition were measured using an MTS assay. ***, $P < 0.001$ *versus* supernatant from ECs. $n = 5$. B. ECs under each condition were also assessed for capillary-like structure formation (top row: "6 h") and migration (bottom two rows: "0 h" and "24 h") and representative images are shown. For the capillary-like formation assay, ECs were seeded, allowed to incubate for 6 h, and then visualized under an Olympus microscope. Black arrows indicate capillary-like structure. To assess migration distance, ECs were visualized by microscope "0 h", then treated for another 24 h, and visualized again ("24 h"). Migration distance was compared before and after treatment. C, D. Show the quantification of these results. ****, $P < 0.0001$. $n = 5$.

Discussion

In this study, we investigated the characteristics of cardiac TCs in a rat model. Our experiments performed *in vitro* demonstrated that TCs can be isolated from the rat heart and cultured in primary cultures, and that the morphology of these cells is consistent with their typical form. Using a combination of different antibodies, stains, and imaging techniques, we were able to visualize cardiac TCs and study their features clearly. Our results showed that TCs form interstitial networks with their long, unique Tps, and that two cardiac TCs can interact through direct contact along the longitudinal axis of the cell body. When dyed with methylene blue, cardiac TCs presented typical moniliform Tps *in vitro*. In addition, when mitochondria were labeled with Janus Green B staining and MitoTracker green, we observed that mitochondria were located in both the cell body and in Tps. Our finding that mitochondria are distributed throughout the entire cell may be indicative of cardiac TC functions, as it implies that TCs are highly active and consume high levels of energy.

Using fluorescence microscopy, our study showed that TCs positively express CD34, C-Kit, and vimentin. Interestingly, when cells were double-labeled there was more co-expression of CD34 and vimentin than of c-Kit and vimentin. Previous studies have confirmed that TCs can be labeled with certain antibodies [20, 21], and a few markers are currently verified as being accurate labels of TCs. At present, the

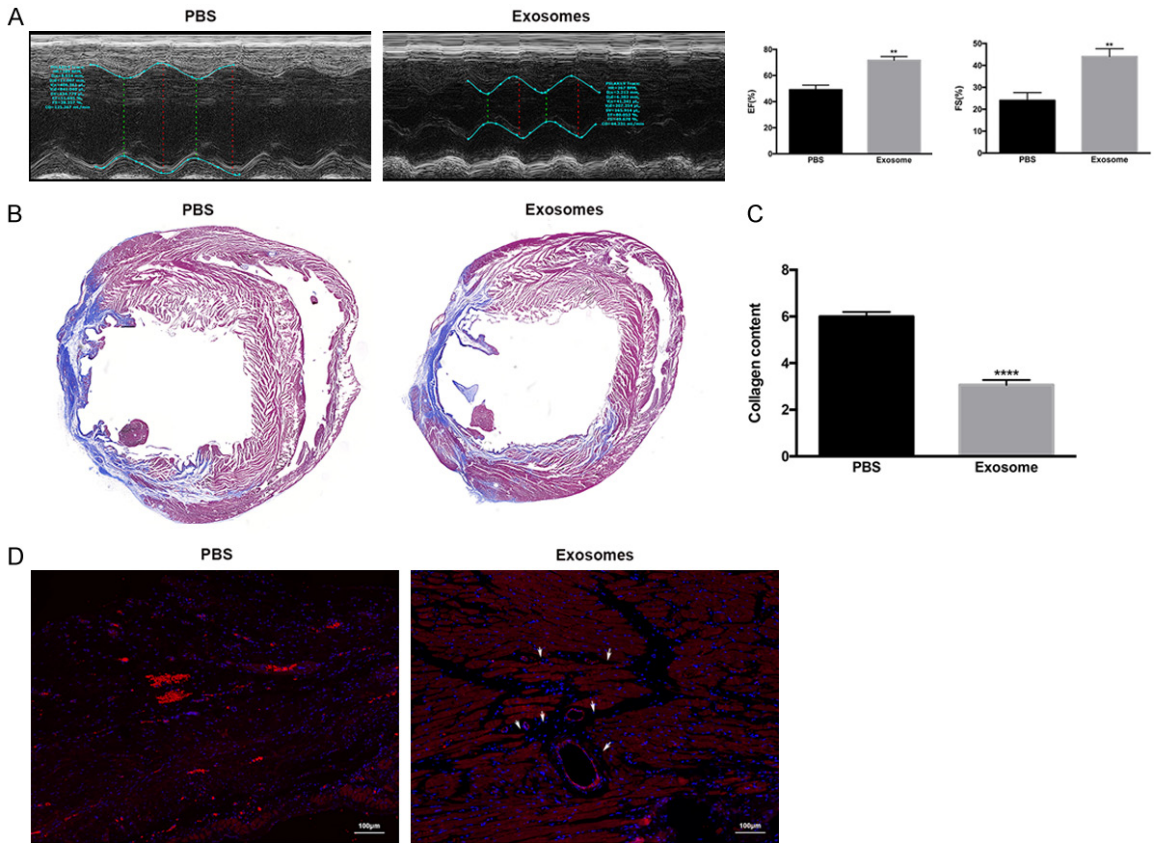

Figure 6. Transfer of exosomes improved cardiac function, attenuated cardiac fibrosis, and increased angiogenesis following induction of myocardial infarction (MI) in rats. Exosomes or PBS were injected 30 min prior to MI induction, and then three additional injections were given on days 2, 4, and 6 after MI. A. Cardiac function was evaluated 28 days after treatment by echocardiography and measurements of the ejection fraction (EF) and fraction shortening (FS) were performed. **, $P < 0.01$ *versus* PBS group. $n = 10$ for each group. B. Rats were euthanized and the hearts were excised for histological analysis. Representative images are shown for the Masson stain, which showed a decreased cardiac fibrosis area in exosome-treated animals. C. A collagen content assay was performed for both groups, and showed decreased collagen formation in the exosome group. ****, $P < 0.0001$ *versus* PBS group. D. Samples were stained for CD31 (red) and DAPI (blue), and representative images are shown for both groups. Increased staining for CD31 was identified in the exosome-treated group. White arrows indicate neo-angiogenesis. Scale bar: 100 μm.

most reliable of these markers is thought to be CD34 [8, 22], which is a highly glycosylated transmembrane glycoprotein. Importantly, an increasing number of studies have shown that CD34 serves an important role in mediating cell adhesion and participates in the migration and positioning of hematopoietic stem cells involved in inflammation and lymphocyte homing, and a study by Cismasiu and colleagues [23] reported a similar biological function for TCs.

While several protocols are employed to isolate and purify exosomes, characterizing them is strongly based on electron microscopy (size and shape) and western blotting for the existence of protein markers that are involved in exosomal biogenesis such as Alix, TSG101 and/or exosomal membrane molecules such as HSP90, CD9, CD63 and CD81 [24]. Calnexin, an endoplasmic reticulum protein, was detectable in whole cell lysates but absent in the exosomes, indicating that the exosome preparations were not contaminated with other vesicles [25]. β-actin was also absent in the exosomes. Because β-actin was a part of cellular cytoskeleton which didn't exist in exosomes [26, 27]. Furthermore, using TEM, we found that TCs actively secrete exosomes. Exosomes are round, natural nanovesicles that range from 30 to 200 nm in diameter and originate from endosomes. Exosomes are secreted from

the plasma membrane and can be found in most biological fluids, including cultured cell media [28]. Intercellular transfer of exosomes is a well-established mechanism that mediates cell-cell communication [29, 30]. Other transportation modes are by microparticles such as microvesicles and apoptotic bodies. The chief functions of these microparticles are intercellular communication and transportation of various bioactive components (DNA, RNA, miRNA, cytokines, and other proteins). Microvesicles are slightly larger vesicles (100-4000 μm diameter) generated from cells via outward budding and blebbing of the plasma membrane. Microvesicles are secreted by different cell types such as neurons, muscle cells, inflammatory cells, and tumor cells. However, platelets are considered to be major sources of microvesicle production and secretion [31]. Finally, apoptotic bodies are the largest microparticles that are shed from cells during apoptosis [32, 33].

In recent years, the therapeutic effects of exosomes derived from stem cells have been investigated intensely in multiple disease models, and show that these exosomes exert functions similar to those of stem cells, including promoting cutaneous wound healing [34] and reducing the size of MI [35]. However, to date, few studies have aimed to determine the functional role of exosomes derived from TCs in angiogenesis. In this study, we frequently observed exosomes in the immediate vicinity of pits, which suggests that the endocytosis of these vesicles may be how exosomes pass messages from one cell to another. Thus, we isolated exosomes from TCs and evaluated their functions. Since it has been reported that TCs have proangiogenic effects [16], we hypothesized that exosomes from TCs would exert a positive influence on ECs. When we cultured ECs in the presence of exosomes isolated from TCs, we observed increased proliferation, migration, and formation of capillary-like structures by the ECs, and these effects were attenuated when exosomes were first depleted. Then, we evaluated the effects of exosomes *in vivo* by transferring them into MI-induced rats. In these experiments, we observed decreased cardiac fibrosis, increased angiogenesis, and improved cardiac function.

Future studies, perhaps based on biochemical methods, are necessary to further investigate which components of exosomes are important in intercellular communication between cardiac TCs with ECs, as well as the underlying mechanisms. Moreover, our results offer preliminary evidence that cardiac TCs might have therapeutic potential that could be utilized for the design of cell-based cardiac repair strategies.

Acknowledgements

This work was supported by a grant from the Nature Science Foundations of China Grant (NO.81170124). The funders had no role in study design, data collection and analysis, the decision to publish, or preparation of the manuscript.

Disclosure of conflict of interest

None.

Address correspondence to: Drs. Jie Yang and Song Zhang, Department of Cardiovascular Diseases, Xinhua Hospital, School of Medicine, Shanghai Jiaotong University, 1665 Kongjiang Street, Shanghai 200092, P. R. China. Tel: +86 18615821604274; E-mail: jaly666666@hotmail.com (JY); Tel: +86 13916013975; E-mail: zhangsong3961@xinhuamed.com.cn (SZ)

References

[1] Popescu LM, Ciontea SM and Cretoiu D. Interstitial Cajal-like cells in human uterus and fallopian tube. Ann N Y Acad Sci 2007; 1101: 139-165.

[2] Zheng Y, Li H, Manole CG, Sun A, Ge J and Wang X. Telocytes in trachea and lungs. J Cell Mol Med 2011; 15: 2262-2268.

[3] Popescu LM, Gherghiceanu M, Suciu LC, Manole CG and Hinescu ME. Telocytes and putative stem cells in the lungs: electron microscopy, electron tomography and laser scanning microscopy. Cell Tissue Res 2011; 345: 391-403.

[4] Popescu LM, Manole E, Serboiu CS, Manole CG, Suciu LC, Gherghiceanu M and Popescu BO. Identification of telocytes in skeletal muscle interstitium: implication for muscle regeneration. J Cell Mol Med 2011; 15: 1379-1392.

[5] Gherghiceanu M and Popescu LM. Interstitial Cajal-like cells (ICLC) in human resting mammary gland stroma. Transmission electron microscope (TEM) identification. J Cell Mol Med 2005; 9: 893-910.

[6] Suciu L, Popescu LM, Gherghiceanu M, Regalia T, Nicolescu MI, Hinescu ME and Faussone-

Pellegrini MS. Telocytes in human term placenta: morphology and phenotype. Cells Tissues Organs 2010; 192: 325-339.
[7] Manetti M, Guiducci S, Ruffo M, Rosa I, Faussone-Pellegrini MS, Matucci-Cerinic M and Ibba-Manneschi L. Evidence for progressive reduction and loss of telocytes in the dermal cellular network of systemic sclerosis. J Cell Mol Med 2013; 17: 482-496.
[8] Popescu LM and Faussone-Pellegrini MS. TELOCYTES-a case of serendipity: the winding way from interstitial cells of cajal (ICC), via interstitial cajal-like cells (ICLC) to telocytes. J Cell Mol Med 2010; 14: 729-740.
[9] Gherghiceanu M, Manole CG and Popescu LM. Telocytes in endocardium: electron microscope evidence. J Cell Mol Med 2010; 14: 2330-2334.
[10] Bani D, Formigli L, Gherghiceanu M and Faussone-Pellegrini MS. Telocytes as supporting cells for myocardial tissue organization in developing and adult heart. J Cell Mol Med 2010; 14: 2531-2538.
[11] Kostin S. Myocardial telocytes: a specific new cellular entity. J Cell Mol Med 2010; 14: 1917-1921.
[12] Gherghiceanu M and Popescu LM. Heterocellular communication in the heart: electron tomography of telocyte-myocyte junctions. J Cell Mol Med 2011; 15: 1005-1011.
[13] Manole CG, Cismasiu V, Gherghiceanu M and Popescu LM. Experimental acute myocardial infarction: telocytes involvement in neo-angiogenesis. J Cell Mol Med 2011; 15: 2284-2296.
[14] Gherghiceanu M and Popescu LM. Cardiac telocytes-their junctions and functional implications. Cell Tissue Res 2012; 348: 265-279.
[15] Popescu L, Gherghiceanu M and Kostin S. Telocytes and heart renewing. In: Wang P, Kuo CH, Takeda N, Singal PK, editors. Adaptation biology and medicine. New Delhi, India: Narosa Publishing House Pvt. Ltd; 2010. pp. 17-39.
[16] Zhao B, Chen S, Liu J, Yuan Z, Qi X, Qin J, Zheng X, Shen X, Yu Y, Qnin TJ, Chan JY and Cai D. Cardiac telocytes were decreased during myocardial infarction and their therapeutic effects for ischaemic heart in rat. J Cell Mol Med 2013; 17: 123-133.
[17] Gherghiceanu M and Popescu LM. Cardiomyocyte precursors and telocytes in epicardial stem cell niche: electron microscope images. J Cell Mol Med 2010; 14: 871-877.
[18] Malik ZA, Kott KS, Poe AJ, Kuo T, Chen L, Ferrara KW and Knowlton AA. Cardiac myocyte exosomes: stability, HSP60, and proteomics. Am J Physiol Heart Circ Physiol 2013; 304: H954-965.
[19] Yu B, Zhang X and Li X. Exosomes derived from mesenchymal stem cells. Int J Mol Sci 2014; 15: 4142-4157.
[20] Gangenahalli GU, Singh VK, Verma YK, Gupta P, Sharma RK, Chandra R and Luthra PM. Hematopoietic stem cell antigen CD34: role in adhesion or homing. Stem Cells Dev 2006; 15: 305-313.
[21] Kim JH, Choi SC, Park CY, Park JH, Choi JH, Joo HJ, Hong SJ and Lim DS. Transplantation of Immortalized CD34+ and CD34-adipose-derived stem cells improve cardiac function and mitigate systemic pro-inflammatory responses. PLoS One 2016; 11: e0147853.
[22] Vannucchi MG, Traini C, Guasti D, Del Popolo G and Faussone-Pellegrini MS. Telocytes subtypes in human urinary bladder. J Cell Mol Med 2014; 18: 2000-2008.
[23] Cismasiu VB and Popescu LM. Telocytes transfer extracellular vesicles loaded with microRNAs to stem cells. J Cell Mol Med 2015; 19: 351-358.
[24] Mathivanan S, Fahner CJ, Reid GE and Simpson RJ. ExoCarta 2012: database of exosomal proteins, RNA and lipids. Nucleic Acids Res 2012; 40: D1241-1244.
[25] Xiao D, Ohlendorf J, Chen Y, Taylor DD, Rai SN, Waigel S, Zacharias W, Hao H and McMasters KM. Identifying mRNA, microRNA and protein profiles of melanoma exosomes. PLoS One 2012; 7: e46874.
[26] Kim HS, Choi DY, Yun SJ, Choi SM, Kang JW, Jung JW, Hwang D, Kim KP and Kim DW. Proteomic analysis of microvesicles derived from human mesenchymal stem cells. J Proteome Res 2012; 11: 839-849.
[27] Dominguez R and Holmes KC. Actin structure and function. Annu Rev Biophys 2011; 40: 169-186.
[28] Keller S, Sanderson MP, Stoeck A and Altevogt P. Exosomes: from biogenesis and secretion to biological function. Immunol Lett 2006; 107: 102-108.
[29] Lu A and Pfeffer SR. A CULLINary ride across the secretory pathway: more than just secretion. Trends Cell Biol 2014; 24: 389-399.
[30] Mittelbrunn M and Sanchez-Madrid F. Intercellular communication: diverse structures for exchange of genetic information. Nat Rev Mol Cell Biol 2012; 13: 328-335.
[31] Boon RA and Vickers KC. Intercellular transport of microRNAs. Arterioscler Thromb Vasc Biol 2013; 33: 186-192.
[32] Zernecke A, Bidzhekov K, Noels H, Shagdarsuren E, Gan L, Denecke B, Hristov M, Koppel T, Jahantigh MN, Lutgens E, Wang S, Olson EN, Schober A and Weber C. Delivery of microRNA-126 by apoptotic bodies induces CXCL12-dependent vascular protection. Sci Signal 2009; 2: ra81.
[33] Kosaka N, Iguchi H, Yoshioka Y, Takeshita F, Matsuki Y and Ochiya T. Secretory mechanisms and intercellular transfer of microRNAs

in living cells. J Biol Chem 2010; 285: 17442-17452.

[34] Zhang J, Guan J, Niu X, Hu G, Guo S, Li Q, Xie Z, Zhang C and Wang Y. Exosomes released from human induced pluripotent stem cells-derived MSCs facilitate cutaneous wound healing by promoting collagen synthesis and angiogenesis. J Transl Med 2015; 13: 49.

[35] Chen L, Wang Y, Pan Y, Zhang L, Shen C, Qin G, Ashraf M, Weintraub N, Ma G and Tang Y. Cardiac progenitor-derived exosomes protect ischemic myocardium from acute ischemia/reperfusion injury. Biochem Biophys Res Commun 2013; 431: 566-571.